

Article

Adsorption of NO Gas Molecules on Monolayer Arsenene Doped with Al, B, S and Si: A First-Principles Study

Keliang Wang ^{1,*} , Jing Li ^{1,*} , Yu Huang ², Minglei Lian ¹ and Dingmei Chen ¹¹ College of Chemistry and Materials Engineering, Liupanshui Normal University, Liupanshui 553004, China² College of Chemistry and Chemical Engineering, Guizhou University, Guiyang 550025, China

* Correspondence: wangkeliang84@163.com (K.W.); woxinfeiyang1986@163.com (J.L.);

Tel.: +86-858-860-0172 (K.W. & J.L.)

Received: 20 July 2019; Accepted: 9 August 2019; Published: 15 August 2019



Abstract: The structures and electronic properties of monolayer arsenene doped with Al, B, S and Si have been investigated based on first-principles calculation. The dopants have great influences on the properties of the monolayer arsenene. The electronic properties of the substrate are effectively tuned by substitutional doping. After doping, NO adsorbed on four kinds of substrates were investigated. The results demonstrate that NO exhibits a chemisorption character on Al-, B- and Si-doped arsenene while a physisorption character on S-doped arsenene with moderate adsorption energy. Due to the adsorption of NO, the band structures of the four systems have great changes. It reduces the energy gap of Al- and B-doped arsenene and opens the energy gap of S- and Si-doped arsenene. The large charge depletion between the NO molecule and the dopant demonstrates that there is a strong hybridization of orbitals at the surface of the doped substrate because of the formation of a covalent bond, except for S-doped arsenene. It indicates that Al-, B- and Si-doped arsenene might be good candidates as gas sensors to detect NO gas molecules owing to their high sensitivity.

Keywords: arsenene; doping; first principles study; gas adsorption; two-dimensional

1. Introduction

Owing to the adequate preparation of single-layer graphene, the research on two-dimensional (2D) materials has been increasing. Graphene, silicene, germanene, hexagonal boron nitride (h-BN), phosphorene, transition metal dichalcogenide and stanine [1–3] have attracted more and more attention in recent years. Especially, because of their ultrathin thickness and high surface-to-volume ratio, atomically thin 2D nanomaterials have been proven to be prospected nanoscale in catalyst, gas sensors and energy storage [4–6].

Good gas sensors for the detection of toxic gas plays a crucial role in industries, chemical detection and environment protection [7–9]. Due to the excellent structural properties of 2D materials, it has attracted wide attention in the field of gas sensors. Ma et al. [10] studied the small molecules (CO, H₂O, NH₃, N₂, NO₂, NO and O₂) adsorbed on the InSe monolayer and found that 2D InSe nanomaterials is a potential candidate for fabricating gas sensors. The study of Liang et al. [11] showed that the affinity between Ga-doped graphene and gas molecules is stronger than that of pristine graphene. For the adsorption of NO_x gases, there have been some experimental studies. MoS₂ nanosheets, prepared by the micromechanical exfoliation method, show a high selectivity for NO_x and NH₃ gas molecules at the ppb level [12,13]. Schedin et al. [14] have researched the adsorption of NO₂, NH₃, H₂O and CO gas molecules on graphene-based gas sensors and found that graphene was electronically quiet enough to be used as a single electronic detector at room temperature.

Recently, monolayer arsenene was predicted to be indirect semiconductors based on its excellent properties of high stability and wide band gaps [15,16]. Similar to silicene, arsenene possesses buckled honeycomb structures [17]. Liu et al. [18] have researched the adsorption of six kinds of small gas molecules on the pristine arsenene monolayer and found that in gas sensing, arsenene can be a potential candidate applied for NO and NO₂ molecules with electrical and magnetic methods. Khan and his coworkers [19] have reported NH₃ and NO₂ molecules show a significant affinity for arsenene leading to strong physisorption.

Generally, doping can improve the adsorption ability of 2D materials to gas molecules [20]. For arsenene doping, the adsorption energy of NH₃ can be enhanced by Ge- and Se-doping [21]. Bai et al. [22] have investigated the structures and properties of monolayer arsenene doped with Ge, Ga, Sb and P, and the results demonstrated that monolayer arsenene doped with Ga changes into the direct band gap. Chen et al. [23] have calculated the adsorption properties of NO₂ and SO₂ on different types of pristine, boron- and nitrogen-doped arsenene, and found that N-doped arsenene is more suitable for SO₂ gas sensors as well as that P-doped arsenene has more potential application in NO₂ gas sensors.

In this paper, we investigated the structures and electronic properties of monolayer arsenene doped with Al, B, S and Si theoretically based on the first-principles calculation. After doping, NO adsorbed on four kinds of substrates were investigated. The adsorption energy, adsorption distance and Mulliken charge transfer were calculated. These results can support a theoretical foundation to design gas sensors using 2D arsenic materials.

2. Computational Methods

The first-principles study, based on density functional theory (DFT), was calculated through the DMol³ code. The generalized gradient approximation (GGA) with the Perdew–Burke–Ernzerhof (PBE) functional [18,19,22] was adopted in the simulation. However, GGA ignores the long-range electron effects, which led to the overestimation of van der Waals forces [24–27]. Therefore, the Grimme custom method was used to describe tiny van der Waals interaction [23,28]. Double numerical atomic orbital plus polarization (DNP) was selected as the basis set to expand electronic wave function. A $4 \times 4 \times 1$ supercell containing 32 atoms was adopted with a vacuum space of 20 Å to guarantee there was no interaction between adjacent layers. An $8 \times 8 \times 1$ and $16 \times 16 \times 1$ k-points in the Brillouin zone were adopted to optimize the configurations and calculate the electronic properties, respectively [19,21]. The convergence tolerance for energy minimizations was 1.0×10^{-6} Ha, for maximum force it was 0.002 Ha/Å and for geometry optimizations it was 0.005 Å, respectively. The flow chart of the computational process is shown in Figure 1.

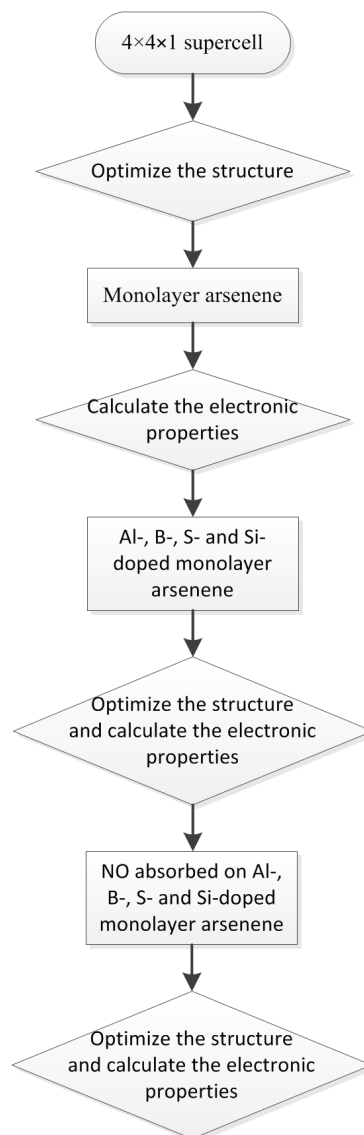


Figure 1. The flow chart of the computational process.

3. Result and Discussion

The structure and electronic properties of pristine monolayer arsenene is firstly tested to check the accuracy of the calculation procedure. The full relaxed lattice constant of monolayer arsenene is 3.624 Å, which is very close to the experimental data [29]. It can be seen from Figure 2a that the bond length of As–As and the bond angle are 2.524 Å and 91.751°, respectively. The thickness of monolayer arsenene is 1.412 Å. The monolayer arsenene with an indirect band gap of 1.718 eV shows a semiconductor property, in which the valence band maximum (VBM) displays at Γ point and the conduction band minimum (CBM) displays between M and Γ point. The results agree well with the previous results [18,22,30,31]. These results verify the accuracy of the calculation procedure and the characterization of the material. Simultaneously, it can be seen from Figure 2b that the partial density of states (PDOS) of the supercell of arsenene, which is mainly dominated by s and p orbitals of As atoms, but the influence on the total density of states (DOS) of the p orbital is greater than that of the s orbital. Similar to the feature of blue phosphorene and silicene [22,32], the energy region near the Fermi level is mainly due to the p orbital of As atoms.

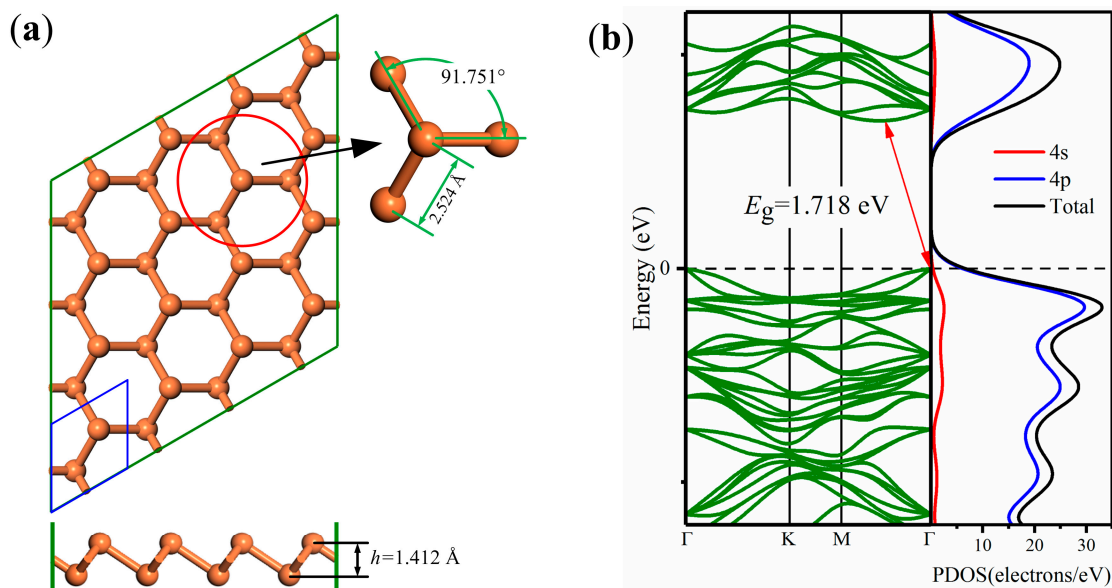


Figure 2. (a) Optimized structure of monolayer arsenene. The blue and green boxes in the top view (top panel) show the primitive cell and the 4×4 supercell, respectively. The buckling height (h) is indicated in the side view (bottom panel). (b) Electronic band structure (left panel) and partial density of states (PDOS) (right panel) of the 4×4 supercell of monolayer arsenene. The Fermi energy was set to zero.

Substitutional doping can effectively improve the adsorption ability of 2D materials to gas molecules. So, the structures and electronic properties of X-doped monolayer arsenene ($X = \text{Al, B, S, Si}$) have been firstly optimized and calculated. The binding energy (E_b) is calculated and defined as $E_b = [E_{X-\text{As}} - (n - 1)E_{\text{As}} - E_X]/n$, where $E_{X-\text{As}}$ is the total energy of substitutional systems, E_{As} and E_X are the energies of the isolated atom As and the dopant atom X, respectively, and n is the number of As atoms in arsenene supercell. It can be seen from the above equation that the greater the binding force between doping elements and the substrate, the more negative the value of E_b . As shown in Table 1, the bond length $l_{X-\text{As}}$ between the dopant X and the nearest As element is in the range of 2.064 to 2.459 Å, and $l_{\text{B-As}}$ is the shortest with 2.064 Å. The binding strength increases in the order of $\text{S} < \text{Al} < \text{Si} < \text{B}$ with high binding energy of -4.065 eV, -4.085 eV, -4.108 eV and -4.137 eV, respectively. It indicates that S, Al, Si and B can interact strongly with its neighboring As atoms. The above results show that the dopants can effectively affect the binding energy for the doped monolayer arsenene.

Table 1. The binding energy (E_b), energy gap (E_g), Mulliken population (Q) and the bond length of X-As ($l_{X-\text{As}}$). A positive Q value means the electrons move from the dopant to the substrate. X denotes the dopant atom.

System	E_b (eV)	E_g (eV)	Q (e)	$l_{X-\text{As}}$ (Å)
Al-doped	-4.085	1.538	0.807	2.429
B-doped	-4.137	1.370	0.175	2.068
S-doped	-4.065	0	-0.120	2.447
Si-doped	-4.108	0	0.665	2.408

Meanwhile, Mulliken analysis is used to calculate the atomic charge near the dopant X and the calculated results are listed in Table 1. The Mulliken population of Al, B, S and Si atoms are 0.807, 0.175, -0.120 and 0.665 e, respectively. The results show that a large amount of electrons transfer occurs between the dopant and the substrate, which implies that there are strong interactions between the dopant and the substrate. The electrons transfer from the dopant to the substrate except for the S atom, because the S atom has a higher electronegativity than that of the As atom. Among these structures, the values of the Mulliken population of Al, B and Si atoms are positive. This leads to the formation

of a huge electron depletion layer on the substrate, which is conducive to improving the adsorption properties for NO gas molecules.

The optimized adsorption configurations of NO adsorbed on four doped systems are demonstrated in Figure 3. The corresponding parameters are listed in Table 2, including the adsorption energy (E_{ad}), adsorption distance (d) and Mulliken charge (Q). It can be seen from Figure 3 that the N atom is toward the substrate and the O atom is away from the substrate in four doped systems. E_{ad} is defined as $E_{ad} = E_{NO/X-As} - (E_{X-As} + E_{NO})$, where $E_{NO/X-As}$, E_{X-As} and E_{NO} denote the total energies of the NO molecule adsorbed on the doped system, the isolated doped substrate and the NO molecule with the same lattice parameters, respectively. The more negative E_{ad} is, the more stable the structure is. B-doped arsenene has the largest adsorption energy of -1.884 eV and the shortest adsorption distance of 1.428 Å with the NO molecule. For Al-, S- and Si-doped arsenene, the adsorption energy values are -1.157 eV, -0.469 eV and -1.586 eV, and the adsorption distance values are 1.942 Å, 2.548 Å and 1.864 Å, respectively. It is clear that the adsorption of NO on S-doped arsenene is physical adsorption and NO on Al-, B- and Si-doped arsenene is chemical adsorption. Mulliken population analysis is performed and the negative Q value indicates electron transfer from the substrates to the NO molecule. It shows that the NO molecule is an electron acceptor with four substrates.

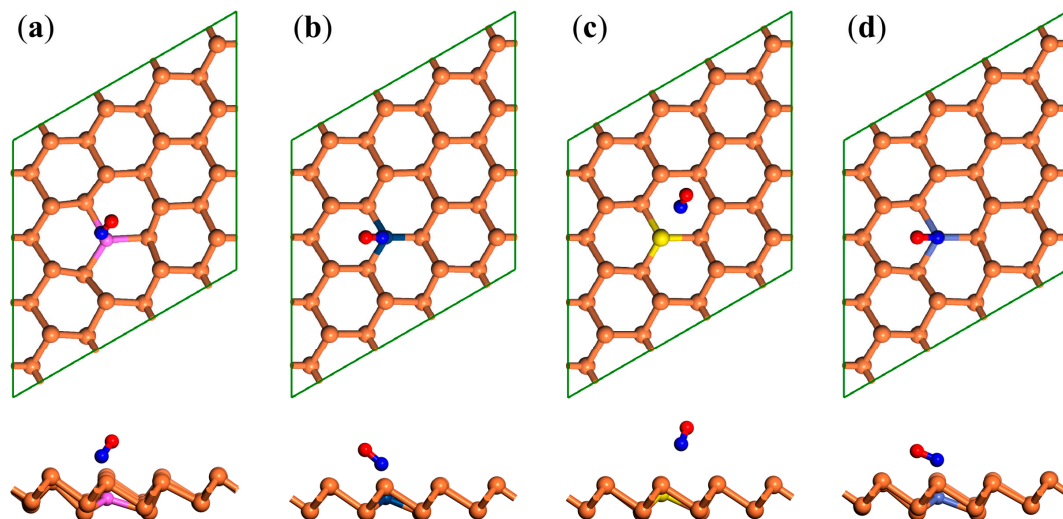


Figure 3. Top view and side view of the most energetically favorable adsorption configurations for NO adsorbed on (a) Al-, (b) B-, (c) S- and (d) Si-doped monolayer arsenene. The O and N atoms are labeled red and blue, respectively.

Table 2. Adsorption energy (E_{ad}), the shortest distance of the As-dopant atom (d) and Mulliken charge (Q) for the optimized stable configurations of gas molecules on Al-, B-, S- and Si-doped arsenene. A negative Q value indicates electron move from the doped substrates to NO molecule.

System	E_{ad} (eV)	d (Å)	Q (e)
Al-doped	-1.157	1.942	-0.184
B-doped	-1.884	1.428	-0.063
S-doped	-0.469	2.548	-0.002
Si-doped	-1.586	1.864	-0.327

Furthermore, the band structures of Al-, B-, S- and Si- doped monolayer arsenene are also calculated to investigate the effects introduced by the dopant. As shown in Figure 4a,b, the dopants of Al and B change the 2D material to the direct band gap from the indirect band gap. Both CBM and VBM are displayed on the Γ point in Brillouin Zone with the values of the band gap 1.538 and 1.370 eV, respectively. The Fermi level of S- and Si-doped arsenene systems enter into the conduction band (see Figure 4c,d) and a semiconductor-metal transition is realized. Through the band structures comparison

of four doped systems, it can be concluded that the electronic properties of 2D materials are effectively tuned by substitutional doping.

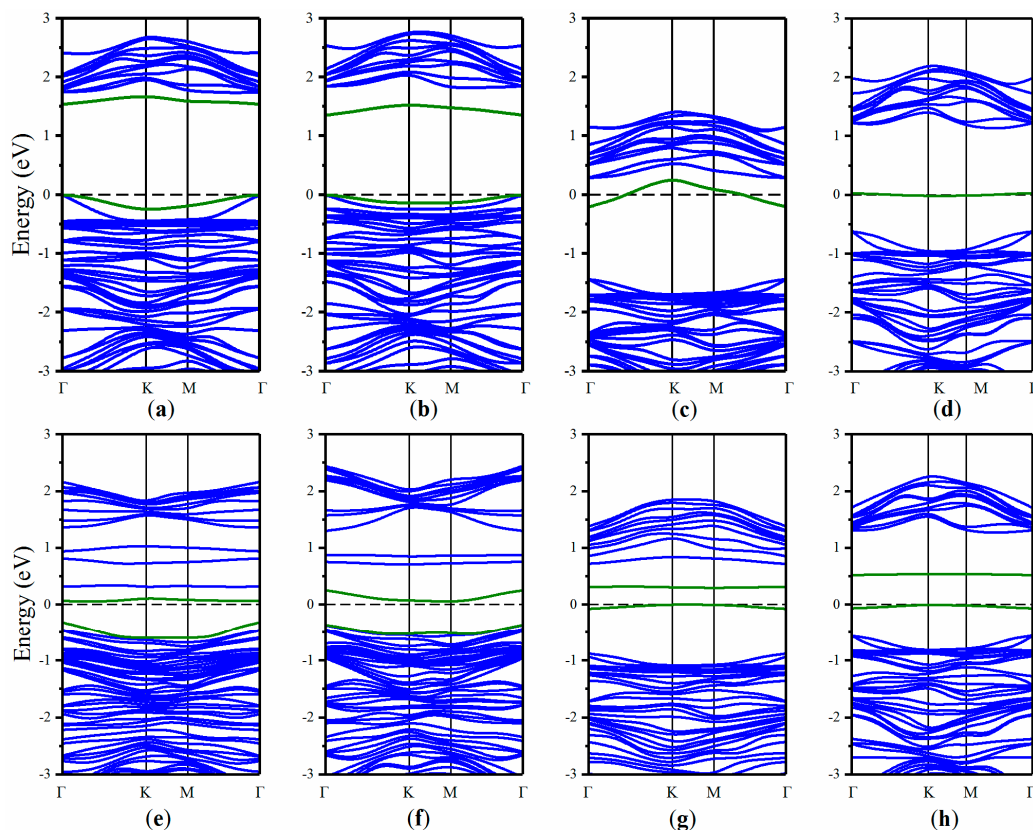


Figure 4. Band structures of (a) Al-, (b) B-, (c) S- and (d) Si-doped arsenene $As_{31}X$ systems, as well as NO adsorbed on (e) $As_{31}Al$, (f) $As_{31}B$, (g) $As_{31}S$ and (h) $As_{31}Si$ monolayers, respectively. The Fermi level is set to zero with the black dashed line.

As can be seen from Figure 4e–h, the band structures of four systems have great changes after the adsorption of the NO molecule. Interestingly, the energy gap values of NO/Al-doped arsenene and NO/B-doped arsenene both change to 0.372 and 0.407 eV, and the energy gap values of NO/S-doped arsenene and NO/Si-doped arsenene change to 0.294 and 0.521 eV. The adsorption of the NO molecule reduces the energy gap of Al- and B-doped arsenene and opens the energy gap of S- and Si-doped arsenene.

To explore the electronic properties of the four systems, the total density of states (DOS) of four systems before and after absorbing the NO molecule were analyzed and shown in Figure 5. Because of the adsorption of NO, the DOS of Al- and B-doped arsenene are shifted to the lower energy level, but the DOS of S- and Si-doped arsenene are shifted slightly to the higher energy level, which are in accordance with the changes of band structures.

To further investigate the NO adsorption on X-doped monolayer arsenene, the charge density differences of NO adsorbed on four kinds of substrates were calculated and shown in Figure 6. The charge density difference can be expressed as $\Delta\rho = \rho_{NO/X-As} - (\rho_{X-As} + \rho_{NO})$, where $\rho_{NO/X-As}$, ρ_{X-As} and ρ_{NO} denote the total charge densities of the optimized NO adsorption system, isolated substrate and NO molecule, respectively. The purple and green parts correspond to the charge accumulation and the charge depletion, respectively. It can be clearly seen that charge redistribution is generated between the NO molecule and the dopant atoms due to the adsorption. The large charge depletion between the NO molecule and the dopant demonstrates that there is a strong hybridization of orbitals at the surface of the doped substrate because of the formation of a covalent bond except for S-doped arsenene. The results are consistent with the Mulliken population analysis.

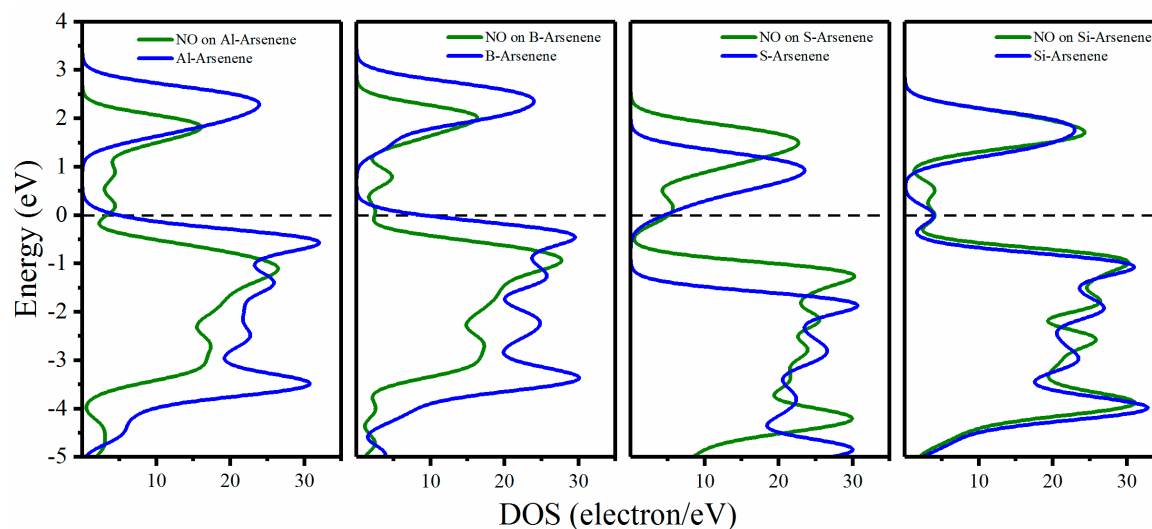


Figure 5. The density of states (DOS) of four systems. Blue and green lines present the DOS of substrates before and after NO adsorption, respectively.

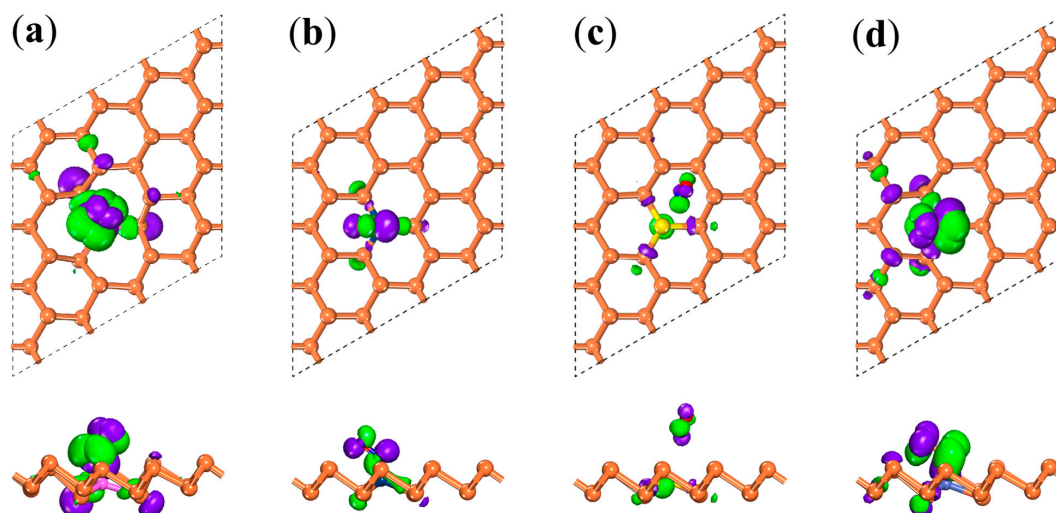


Figure 6. Charge density difference plots for NO adsorbed on (a) Al-, (b) B-, (c) S- and (d) Si-doped monolayer arsenene, respectively. The purple (green) distribution denotes the charge accumulation (depletion) with the isosurface of $0.03 \text{ e}/\text{\AA}^3$ for (a) and (d); $0.044 \text{ e}/\text{\AA}^3$ for (b) and $0.05 \text{ e}/\text{\AA}^3$ for (c).

4. Conclusions

On the basis of first-principles calculation, the structures and electronic properties of monolayer arsenene doped with Al, B, S and Si were investigated. The dopants have great influences on the properties of the monolayer arsenene. The electronic properties of the substrate are effectively tuned by substitutional doping.

After doping, NO adsorbed on four kinds of substrates have been investigated. The NO molecule is an electron acceptor with four substrates. The adsorption energy, adsorption distance and Mulliken charge transfer have been calculated. The results demonstrate that NO exhibits a chemisorption character on Al-, B- and Si-doped arsenene, while a physisorption character on S-doped arsenene with moderate adsorption energy.

Due to the adsorption of NO, the band structures of the four systems have great changes. It reduces the energy gap of Al- and B-doped arsenene and opens the energy gap of S- and Si-doped arsenene. The large charge depletion between the NO molecule and the dopant demonstrates that there is a strong hybridization of orbitals at the surface of the doped substrate because of the formation

of a covalent bond except for S-doped arsenene. It indicates that Al-, B- and Si-doped arsenene might be good candidates as gas sensors to detect NO gas molecules owing to their high sensitivity.

Author Contributions: K.W. and J.L. conceived and designed this case-study as well as wrote the paper; M.L. and D.C. reviewed the paper; all authors interpreted the data; and Y.H. substantively revised the work and contributed the process simulation.

Funding: This work is financially supported by Guizhou Province United Fund (Qiankehe J zi LKLS[2013]27), Excellent engineers education training plan (LPSSY zyypjyh201702), Guizhou Solid Waste Recycling Laboratory of Coal Utilization ([2011]278), the Scientific and Technological Innovation Platform of Liupanshui (52020-2018-03-02) and Academician Workstation of Liupanshui Normal University (qiankehepingtairencai [2019]5604).

Conflicts of Interest: The authors declare no conflict of interest.

References

1. Nagarajan, V.; Bhattacharyya, A.; Chandiramouli, R. Adsorption of ammonia molecules and humidity on germanene nanosheet—a density functional study. *J. Mol. Graph. Model.* **2018**, *79*, 149–156. [[CrossRef](#)] [[PubMed](#)]
2. Komsa, H.; Krasheninnikov, A.V. Electronic structures and optical properties of realistic transition metal dichalcogenide heterostructures from first principles. *Phys. Rev. B* **2013**, *88*, 85318. [[CrossRef](#)]
3. Zhang, S.; Guo, S.; Huang, Y.; Zhu, Z.; Cai, B.; Xie, M.; Zhou, W.; Zeng, H. Two-dimensional SiP: An unexplored direct band-gap semiconductor. *2D Mater.* **2017**, *4*, 15030. [[CrossRef](#)]
4. Yang, W.; Gan, L.; Li, H.; Zhai, T. Two-dimensional layered nanomaterials for gas-sensing applications. *Inorg. Chem. Front.* **2016**, *3*, 433–451. [[CrossRef](#)]
5. Lightcap, I.V.; Kamat, P.V. Graphitic design: Prospects of graphene-based nanocomposites for solar energy conversion, storage, and sensing. *Acc. Chem. Res.* **2012**, *46*, 2235–2243. [[CrossRef](#)] [[PubMed](#)]
6. Zhang, S.; Zhou, W.; Ma, Y.; Ji, J.; Cai, B.; Yang, S.A.; Zhu, Z.; Chen, Z.; Zeng, H. Antimonene oxides: Emerging tunable direct bandgap semiconductor and novel topological insulator. *Nano Lett.* **2017**, *17*, 3434–3440. [[CrossRef](#)]
7. Nagarajan, V.; Chandiramouli, R. Adsorption behavior of NH₃ and NO₂ molecules on stanene and stanane nanosheets—A density functional theory study. *Chem. Phys. Lett.* **2018**, *695*, 162–169. [[CrossRef](#)]
8. Yamazoe, N. Toward innovations of gas sensor technology. *Sens. Actuators B Chem.* **2005**, *108*, 2–14. [[CrossRef](#)]
9. Lagód, G.; Duda, S.M.; Majerek, D.; Szutt, A.; Dołhańczuk-Śródka, A. Application of electronic nose for evaluation of wastewater treatment process effects at full-scale WWTP. *Processes* **2019**, *7*, 251. [[CrossRef](#)]
10. Ma, D.; Ju, W.; Tang, Y.; Chen, Y. First-principles study of the small molecule adsorption on the InSe monolayer. *Appl. Surf. Sci.* **2017**, *426*, 244–252. [[CrossRef](#)]
11. Liang, X.; Ding, N.; Ng, S.; Wu, C.L. Adsorption of gas molecules on Ga-doped graphene and effect of applied electric field: A DFT study. *Appl. Surf. Sci.* **2017**, *411*, 11–17. [[CrossRef](#)]
12. Late, D.J.; Huang, Y.K.; Liu, B.; Acharya, J.; Shirodkar, S.N.; Luo, J.; Rao, C.N. Sensing behavior of atomically thin-layered MoS₂ transistors. *ACS Nano* **2013**, *7*, 4879–4891. [[CrossRef](#)] [[PubMed](#)]
13. Donarelli, M.; Prezioso, S.; Perrozzi, F.; Bisti, F.; Nardone, M.; Giancaterini, L.; Ottaviano, L. Response to NO₂ and other gases of resistive chemically exfoliated MoS₂-based gas sensors. *Sens. Actuators B Chem.* **2015**, *207*, 602–613. [[CrossRef](#)]
14. Schedin, F.; Geim, A.K.; Morozov, S.V.; Hill, E.W.; Blake, P.; Katsnelson, M.I.; Novoselov, K.S. Detection of individual gas molecules adsorbed on graphene. *Nat. Mater.* **2007**, *6*, 652. [[CrossRef](#)] [[PubMed](#)]
15. Zhang, S.; Guo, S.; Chen, Z.; Wang, Y.; Gao, H.; Gómez-Herrero, J.; Ares, P.; Zamora, F.; Zhu, Z.; Zeng, H. Recent progress in 2D group-VA semiconductors: From theory to experiment. *Chem. Soc. Rev.* **2018**, *47*, 982–1021. [[CrossRef](#)] [[PubMed](#)]
16. Zhang, S.; Yan, Z.; Li, Y.; Chen, Z.; Zeng, H. Atomically thin arsenene and antimonene: Semimetal–semiconductor and indirect–direct band-gap transitions. *Angew. Chem.* **2015**, *54*, 3112–3115. [[CrossRef](#)] [[PubMed](#)]
17. Zhang, S.; Xie, M.; Li, F.; Yan, Z.; Li, Y.; Kan, E.; Liu, W.; Chen, Z.; Zeng, H. Semiconducting group 15 monolayers: A broad range of band gaps and high carrier mobilities. *Angew. Chem.* **2016**, *55*, 1666–1669. [[CrossRef](#)]

18. Liu, C.; Liu, C.; Yan, X. Arsenene as a promising candidate for NO and NO₂ sensor: A first-principles study. *Phys. Lett. A* **2017**, *381*, 1092–1096. [[CrossRef](#)]
19. Khan, M.S.; Srivastava, A.; Pandey, R. Electronic properties of a pristine and NH₃/NO₂ adsorbed buckled arsenene monolayer. *RSC Adv.* **2016**, *6*, 72634–72642. [[CrossRef](#)]
20. Xie, M.; Zhang, S.; Cai, B.; Zou, Y.; Zeng, H. N-and p-type doping of antimonene. *RSC Adv.* **2016**, *6*, 14620–14625. [[CrossRef](#)]
21. Khan, M.S.; Ranjan, V.; Srivastava, A. NH₃ adsorption on arsenene: A first principle study. In Proceedings of the 2015 IEEE International Symposium on Nanoelectronic and Information Systems, Indore, India, 21–23 December 2015; IEEE: Piscataway, NJ, USA, 2015; pp. 248–251.
22. Bai, M.; Zhang, W.X.; He, C. Electronic and magnetic properties of Ga, Ge, P and Sb doped monolayer arsenene. *J. Solid State Chem.* **2017**, *251*, 1–6. [[CrossRef](#)]
23. Chen, X.; Wang, L.; Sun, X.; Meng, R.; Xiao, J.; Ye, H.; Zhang, G. Sulfur dioxide and nitrogen dioxide gas sensor based on arsenene: A first-principle study. *IEEE Electron Device Lett.* **2017**, *38*, 661–664. [[CrossRef](#)]
24. Berland, K.; Cooper, V.R.; Lee, K.; Schröder, E.; Thonhauser, T.; Hyldgaard, P.; Lundqvist, B.I. Van der Waals forces in density functional theory: A review of the vdW-DF method. *Rep. Prog. Phys.* **2015**, *78*, 066501. [[CrossRef](#)] [[PubMed](#)]
25. Tamijani, A.A.; Salam, A.; de Lara-Castells, M.P. Adsorption of noble-gas atoms on the TiO₂ (110) surface: An Ab initio-assisted study with van der Waals-corrected DFT. *J. Phys. Chem. C* **2016**, *120*, 18126–18139. [[CrossRef](#)]
26. Grimme, S. Semiempirical GGA-type density functional constructed with a long-range dispersion correction. *J. Comput. Chem.* **2006**, *27*, 1787–1799. [[CrossRef](#)] [[PubMed](#)]
27. Lee, K.; Murray, É.D.; Kong, L.; Lundqvist, B.I.; Langreth, D.C. Higher-accuracy van der Waals density functional. *Phys. Rev. B* **2010**, *82*, 081101. [[CrossRef](#)]
28. Guo, S.; Yuan, L.; Liu, X.; Zhou, W.; Song, X.; Zhang, S. First-principles study of SO₂ sensors based on phosphorene and its isoelectronic counterparts: GeS, GeSe, SnS, SnSe. *Chem. Phys. Lett.* **2017**, *686*, 83–87. [[CrossRef](#)]
29. Schiferl, D.; Barrett, C.S. The crystal structure of arsenic at 4.2, 78 and 299 K. *J. Appl. Crystallogr.* **1969**, *2*, 30–36. [[CrossRef](#)]
30. Kamal, C.; Ezawa, M. Arsenene: Two-dimensional buckled and puckered honeycomb arsenic systems. *Phys. Rev. B* **2015**, *91*, 85423. [[CrossRef](#)]
31. Kecik, D.; Durgun, E.; Ciraci, S. Optical properties of single-layer and bilayer arsenene phases. *Phys. Rev. B* **2016**, *94*, 205410. [[CrossRef](#)]
32. Segall, M.D.; Shah, R.; Pickard, C.J.; Payne, M.C. Population analysis of plane-wave electronic structure calculations of bulk materials. *Phys. Rev. B* **1996**, *54*, 16317–16320. [[CrossRef](#)] [[PubMed](#)]

